

SIMULATION OF CROWD EVACUATION BEHAVIOURS AT SUBWAY STATIONS UNDER PANIC EMOTION

Chen, Y. X.^{*,**,#}; Song, Y. H.^{*,**} & Huo, F. Z.^{*,**}

* School of Safety Science and Emergency Management, Wuhan University of Technology,
Wuhan, 430000, China

** China Research Center for Emergency Management, Wuhan University of Technology,
Wuhan, 430000, China

E-Mail: charlychen@whut.edu.cn (# Corresponding author)

Abstract

To explore companion movement laws of different age groups and transfer rules of panic emotion during evacuation at subway stations, evacuation groups of different ages were distinguished in this study through differences in movement rate. Moreover, a double-exit subway cellular automaton evacuation model considering companion behaviours was constructed. A case study of evacuation of dense crowds at the Hukou Subway in Wuhan City of China was simulated, and effects of personnel structure, companion behaviours, and panic emotion on evacuation efficiency were analysed. Results show that, (1) the overall crowd evacuation time present a linear growth trend with the increase of pedestrian density. (2) The evacuation time initially decreases and then increases with the increase of companion ratio. The shortest evacuation time is achieved when the companion cells account for 10%. (3) People are more reasonable and the general evacuation efficiency is higher if they can control emotions better during evacuation. The obtained conclusions provide great references to analyse companion behaviours of different age groups during evacuation.

(Received in July 2023, accepted in October 2023. This paper was with the authors 1 month for 1 revision.)

Key Words: Evacuation, Companion Behaviour, Movement Rate, Panic Emotion, Cellular Automaton

1. INTRODUCTION

Rail traffic has been extensively applied to traffic transportation in large and middle-sized cities at home and abroad for its high carrying capacity, fast speed, high accuracy, and low energy consumption. By December 2021, rail traffic has been built in 50 cities in China, and operational subway lines have exceeded 100 km in 22 cities. As a major public transport mode, subway has advantages of high passenger capacity and closed space [1]. However, subway stations also have disadvantages, including high crowd density, limited exit setting, and poor ventilation and fresh air circulation. These factors can contribute to the likelihood of secondary safety accidents, such as stampedes, in the event of a subway operational accident. Consequently, countries place significant emphasis on ensuring evacuation safety at subway stations. The United States' NFPA 130 (2014) standard specifies a 4-min evacuation time, whereas Japan's Railway Technical Standards mandate that the evacuation time from subway platform to the surface of the railway station shall be within 10 min. As for China, the GB/T 33668—2017 Subway Safety Evacuation Codes require passengers to reach a safe zone within 6 min.

Subway operation safety accidents are usually divided according to manifestation patterns and causes. According to manifestation patterns, subway operation safety accidents can be divided into 14 types, namely, fire disaster, explosion, suicide, terrorist attack, falling accident, falling into rails, derail, train collision, natural disaster, suffocate, stampede, poisoning, electric shock, and operation interruption. According to causes, subway operation safety accidents can be divided into 14 types, namely, foreign matter invasion, passenger conflict, jam, operation against rules, unsafe acts of passengers, signal fault, communication fault, electrical equipment

failure, vehicle failure, power supply system failure, elevator failure, safety door failure, automatic fare collection system failure, and rail facility failure [2]. Different types of subway operation safety accident have various formation mechanisms. However, whether evacuation can be completed in time upon risks can bring serious safety threats to passengers' life and property. Therefore, finding efficient and safe evacuation methods for stranded passengers during subway accidents has become a key area of research. Currently, crowd evacuation studies in subway scenarios mainly involve software simulation instead of field experiments due to two reasons. First, field experiments are resource-intensive and potentially hazardous, with risks such as stampedes caused by crowd conditions. Second, introducing risk elements such as smoke and poison gas in large-scale crowd evacuations can result in irreversible health damages. Conversely, computer simulation studies can save time, reduce personnel costs, minimize experimental safety risks, accurately simulate changes of risk factors (e.g., smoke, temperature, visibility, heat release rate, and concentration of combustion products), which may exist in experimental environment under the assistance of software such as FDS [3-5]. Therefore, a cellular automaton model was used as the theoretical research basis, and computer simulation was applied to examine the companion movement laws and transmission laws of panic emotion of different age groups during subway evacuation. By comparing crowd evacuation laws under different scenarios, a subway crowd evacuation strategy considering panic factors was proposed to comprehensively improve evacuation efficiency of passengers retained for subway operation safety during emergencies.

2. LITERATURE REVIEW

In traditional cellular automaton model studies, some experts have emphasized on the simulation of behaviours of evacuees based on models, thereby enabling the simulation of evacuation process accurately and comprehensively. Qin et al. [6] proposed an extended cellular automaton model that addresses the issue of traditional methods of setting floor fields could result in significant underuse of exit areas when people converge on one side of the egress. Ciallella et al. [7] discovered that excessive evacuation information might increase information processing cost of the crowd, thereby decreasing information transmission efficiency and lowering evacuation efficiency. Pereira et al. [8] built an extended cellular automaton model based on pedestrian behavioural dynamics to enhance overall crowd evacuation efficiency. Jahedinia et al. [9] found that passengers with luggage occupy extra evacuation space during subway evacuations, leading to slower passenger speed under congested conditions, thereby extending total evacuation time and decreasing evacuation efficiency. Mitsopoulou et al. [10] used a cellular automaton model and combined it with a spatial gaming approach to investigate the influences of conflict events in anxious crowds on the evacuation process. Geng et al. [11] simulated the distribution of memory points of pedestrians, number of memory points, and scope of memory angle by using an improved cellular automaton model, and discussed the evacuation characteristics of crowds under unfavourable visual conditions. Existing studies have mainly investigated crowd behaviour and their anxiety during evacuations based on a cellular automaton model. They aim to reduce congestion during evacuations by analysing crowd evacuation behaviour and their anxiety levels, and these studies have made significant advancements. Nevertheless, the panic emotion, which arises in conjunction with anxiety during evacuations, may also spread. The task of objectively and comprehensively describing the spread of panic in the evacuation process is worthy of further in-depth studies.

Some scholars have focused on quantifying external conditions during evacuations through models and simulating the influences of these conditions on the evacuation process. Helbing et al. [12, 13] developed a social force model and analysed the "fast is slow" and "hunch-up before the exit" evacuation phenomenon, arguing that disordered evacuations may decrease the overall

efficiency. Li et al. [14] studied the influences of crowd distribution on evacuation efficiency, and found that the initial disordered distribution state is superior to ordered distribution state in terms of evacuation efficiency. Gokce et al. [15] and Gwizdalla [16] studied the influences of barriers on the evacuation process, with consistent research results. They found that appropriate barriers in a room could decrease crowding, shorten evacuation times, and increase efficiency. Miyagawa and Ichinose [17] found that the traditional cellular automaton model's representation of evacuees as 1×1 square cells could not reflect the shoulder width accurately. However, 1×2 rectangular cells not only can reflect the shoulder width of evacuees but also increase motion tracks for lateral movement and turning, resulting in a more realistic simulation of evacuee pathways. Zuriguel et al. [18] and Yanasigawa et al. [19] demonstrated through experiments and a floor field model that correctly positioned barriers near exits could decrease crowding and improve overall efficiency. Song et al. [20] combined potential field and cellular automaton concepts to create a smoke diffusion model in closed environments, simulating smoke propagation and pedestrian evacuation conditions. Yi et al. [21] developed an extended floor field model to investigate the dynamic process of pedestrian evacuation during stampede, and analysed influences of pedestrian density, activity site, stampede position, evacuation strategy, occurrence time of stampede, and duration on efficiency and safety. They found that pedestrians should stay away from the stampede position, follow directions of the majority in the perception scope, and walk against the wall. Feliciani and Nishinari [22] proposed an improved cellular automaton floor field model that increases the maximum allowable density in the simulation process using a subgrid system. This model is used to prevent evacuation accidents caused by overloading of people. These research perspectives mainly focus on external factors that influence the evacuation process by using cellular automaton, social force model, and other methods, revealing evacuation field factors (e.g., barriers and evacuation road) on the process. Although these studies have achieved good progresses, they may have overlooked the influence of different age groups' varying moving speeds and interactive behaviours (e.g., hand-in-hand mutual help) during evacuations.

Based on the aforementioned research, existing evacuation studies mainly focus on the influences of anxiety and field factors on the evacuation process. However, studies on panic emotion from feeling of anxiety, movement state in the evacuation process, and interactive behaviours are lacking. Considering this situation, this study conducts extensive groundwork on evacuation at subway areas. The crowd is classified into adult cells, companion cells, disadvantage cells (e.g., children and the old) according to age structure and companion behaviours during evacuation. Moreover, different action time steps are assigned based on the actual walking speed differences. In addition, the panic emotion during evacuation is quantified using the SIS infectious disease dynamics model to simulate evacuation process in a subway environment accurately and comprehensively.

3. METHODOLOGY

3.1 Cellular automaton model of different moving speeds

The Moore neighbourhood was selected to build the model, in which three types of pedestrian were set, including adult cells, disadvantage cells, and companion cells. The first two types of cells could choose one of eight cellular directions surrounding the central one randomly during evacuation (Fig. 1 a). Companion cell is the cellular combination composed of one adult and one disadvantage companion. The companion cell can choose one of eight cellular directions surrounding the central one randomly during evacuation (Fig. 1 b).

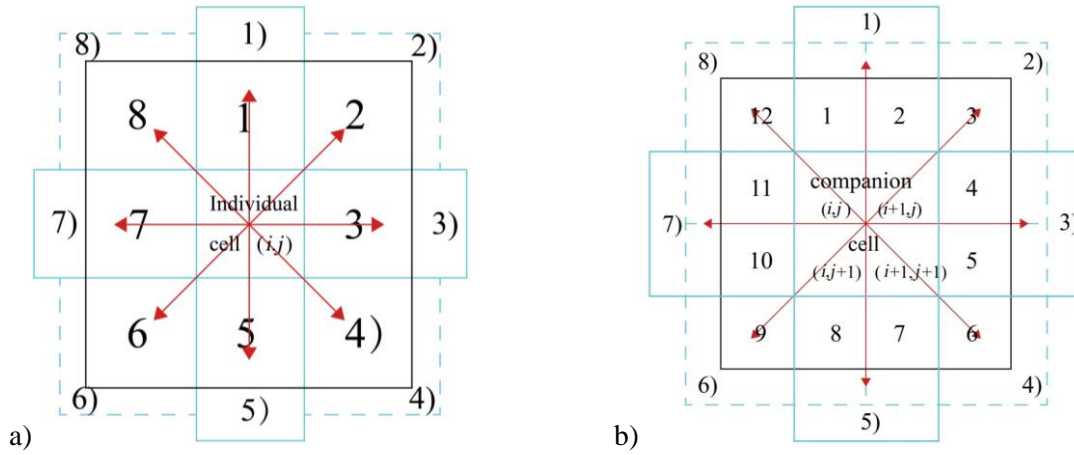


Figure 1: Moving direction of cells; a) adult cell and disadvantage cells, b) companion cells.

In each time step, a cell can only move for the length of a cell or stay static. When two or more pedestrians want to enter into one cell at the same time, the entrance order is determined according to their competitiveness. The companion cell has stronger competitiveness than individual cells, and adult cells have stronger competitiveness than disadvantage cells. If they have the same competitiveness, then one pedestrian is chosen randomly to enter into the cell, while others wait at the initial place.

The transfer probability of the pedestrians is as follows:

$$P_{i,j} = N * \exp(k_s S_{i,j}) * \exp(-k_D D_{i,j}) * \exp(k_M M_{i,j}) (1 - n_{i,j}) (1 - \varepsilon_{i,j}) \quad (1)$$

where N is the normalization coefficient of the $P_{i,j}$. $n_{i,j}$ and $\varepsilon_{i,j}$ are both state parameters of cells. If the cell is occupied by barriers, $n_{i,j} = 1$; otherwise, $n_{i,j} = 0$. If the cell is occupied by a pedestrian, then $\varepsilon_{i,j} = 1$; otherwise, $\varepsilon_{i,j} = 0$. K_s , k_D and k_M are the weight coefficients of different parameters. $S_{i,j}$ is the static field parameter. $D_{i,j}$ is a dynamic field parameter, see Eq. (2). $M_{i,j}$ is a conformity parameter, see Eq. (3).

$D_{i,j}$ is a dynamic field parameter that expresses the repulsive force of risk source to pedestrians. The repulsive force at the point furthest to the risk source along eight movement directions of the cell was set as 0, see Eq. (2).

$$D_{i,j} = \max_{R \in \sqrt{E}} \sqrt{(i_f - i)^2 + (j_f - j)^2} - \sqrt{(i_f - i)^2 + (j_f - j)^2} \quad (2)$$

where (i_f, j_f) is the coordinates of the risk source. (i, j) are the coordinates of the cell.

$M_{i,j}$ is a conformity parameter that expresses the attraction of crowding degree on the target directions of a cell to the pedestrians, see Eq. (3).

For adult cells and disadvantage cells, $m_{i,j}$ in Fig. 1 a is as follows:

Direction 1)	$m_1 = \varepsilon_1 + 0.5(\varepsilon_8 + \varepsilon_2)$	Direction 2)	$m_2 = \varepsilon_2 + 0.5(\varepsilon_1 + \varepsilon_3)$
Direction 3)	$m_3 = \varepsilon_3 + 0.5(\varepsilon_2 + \varepsilon_4)$	Direction 4)	$m_4 = \varepsilon_4 + 0.5(\varepsilon_3 + \varepsilon_5)$
Direction 5)	$m_5 = \varepsilon_5 + 0.5(\varepsilon_4 + \varepsilon_6)$	Direction 6)	$m_6 = \varepsilon_6 + 0.5(\varepsilon_5 + \varepsilon_7)$
Direction 7)	$m_7 = \varepsilon_7 + 0.5(\varepsilon_6 + \varepsilon_8)$	Direction 8)	$m_8 = \varepsilon_8 + 0.5(\varepsilon_7 + \varepsilon_1)$

For companion cells, according to a practical test, $m_{i,j}$ in Fig. 1 b is as follows:

Direction 1)	$m_1 = \varepsilon_1 + \varepsilon_2 + 0.5(\varepsilon_{12} + \varepsilon_3)$	Direction 2)	$m_2 = \varepsilon_2 + \varepsilon_3 + \varepsilon_4$
Direction 3)	$m_3 = \varepsilon_4 + \varepsilon_5 + 0.5(\varepsilon_3 + \varepsilon_6)$	Direction 4)	$m_4 = \varepsilon_5 + \varepsilon_6 + \varepsilon_7$
Direction 5)	$m_5 = \varepsilon_7 + \varepsilon_8 + 0.5(\varepsilon_6 + \varepsilon_9)$	Direction 6)	$m_6 = \varepsilon_8 + \varepsilon_9 + \varepsilon_{10}$
Direction 7)	$m_7 = \varepsilon_{10} + \varepsilon_{11} + 0.5(\varepsilon_9 + \varepsilon_{12})$	Direction 8)	$m_8 = \varepsilon_{11} + \varepsilon_{12} + \varepsilon_1$

$M_{i,j}$ can be calculated as follows:

$$M_{i,j} = \frac{m_{i,j}}{\sum m_{i,j}} = \frac{m_{i,j}}{m_1+m_2+\dots+m_8} = \frac{m_{i,j}}{2\sum \varepsilon} \quad (3)$$

3.2 Movement model of pedestrians under the panic emotion

Existing research has shown that the SIS model can accurately quantify the values of panic emotions in real life [23, 24], and on the other hand, it can demonstrate the transmission patterns of panic emotions during the evacuation process [25, 26]. The susceptible individuals (S) and the infected state (I) convert each other based on the value of the panic emotion (E) during the evacuation process. The panic emotion (E) of each cell in the evacuation process can be calculated according to the following equation:

$$E_{(i,j)}^{t+1} = E_{(i,j)}^t \alpha + \sum_{R \leq \sqrt{2}, E^t \geq E_0} E^t \beta \quad (4)$$

where α is the attenuation coefficient of panic emotion in the evacuation process, β is the transmission coefficient of panic emotion of the infected (I), E_0 is the threshold of panic emotion, R is the radius of the cell, and E^t is the panic value of the cell under the time step (t).

The panic emotion (E) of individuals at the initial moment of evacuation generally obeys to a normal distribution of $N(0.5, \sigma^2)$. Susceptible individuals (S) move by observing the movement laws of Eq. (1). The infected (I) is affected significantly by the panic emotion, preventing them from completing the evacuation process in a reasonable manner. The infected (I) only $k_D D_{i,j}$ is considered in the movement laws of Eq. (1), and $k_s S_{i,j}$ and $k_M M_{i,j}$ are not calculated.

3.3 Cell updating rules

The competitiveness rule is introduced as follows. The companion cell has stronger competitiveness than individual cells, and adult cells have stronger competitiveness in individual cells. When cells have the same competitiveness, the individual is chosen randomly to enter into the unoccupied cell, whereas other cells wait at the same place until the evacuation is finished. The specific updating rule is shown in Fig. 2.

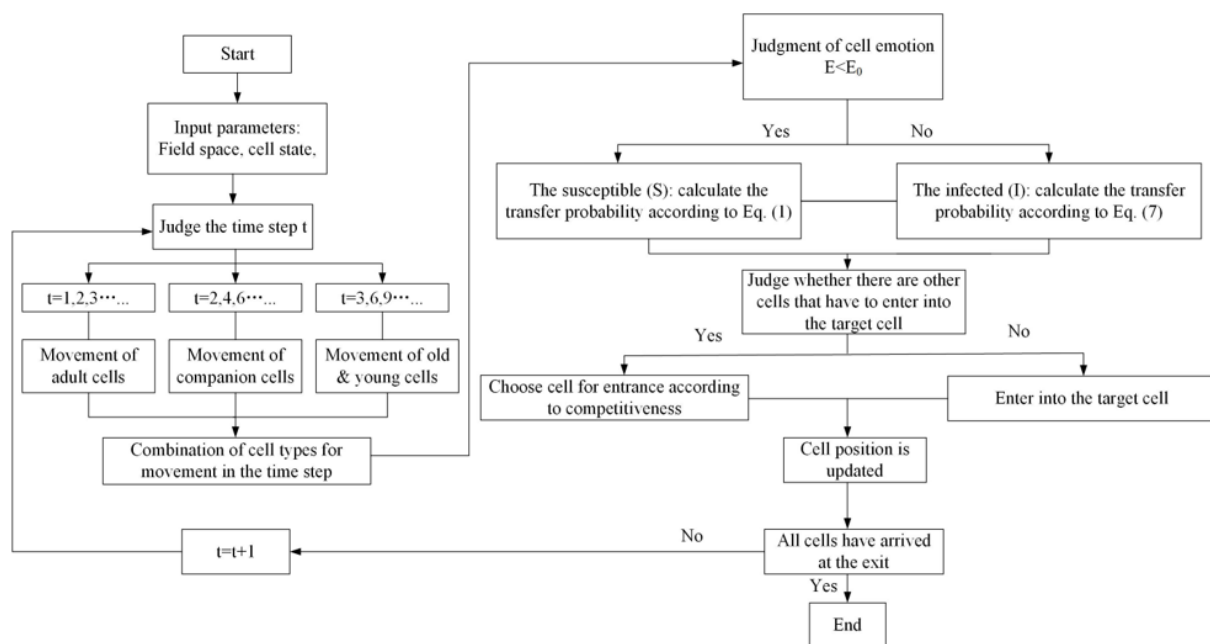


Figure 2: Cellular automaton process considering companion behaviours.

3.4 Simulation of evacuation process

According to a case study based on Hukou Subway Station in Wuhan City, the proportions of three cell types (according to sequence of time step movement) were set as adult cell : companion cell : disadvantage cell = 0.55 : 0.15 : 0.15. To guarantee the effectiveness of the simulation results, 10 tests were performed randomly under various states to eliminate the influence of accidental error on the test results. The platform structure is shown in Fig. 3.

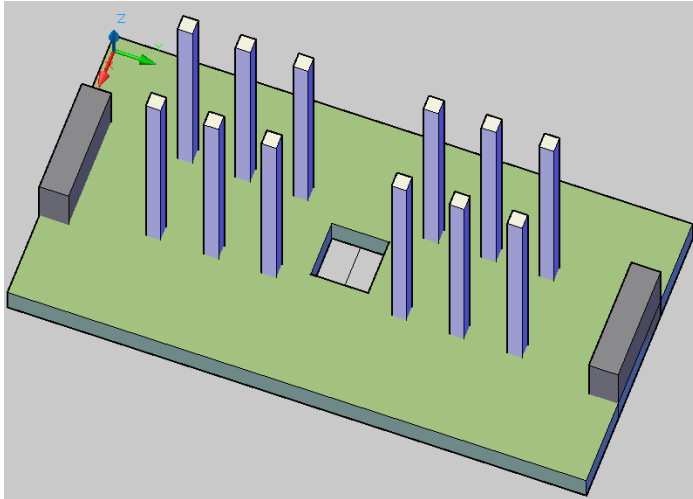


Figure 3: Diagram of subway platform.

To guarantee the effectiveness of the proposed model, k_s , k_D and k_M in Eq. (1) are calculated before simulation. Data were initialized by setting the population density (ρ) at 0.15 to determine the static field coefficient (k_s), dynamic field coefficient (k_D), and conformity parameter (k_M). The test results are shown in Fig. 4.

Static field coefficient (k_s). According to the test results in Fig. 4 a, the evacuation time drops quickly with the increase of k_s in the interval of [1, 1.4], but it increases with k_s in the interval of [1.4, 2]. Thus, the static field coefficient (k_s) is fixed at 1.4 for maximum evacuation efficiency.

Dynamic field coefficient (k_D). Test results in Fig. 4 b show that the evacuation time reduces slowly with the increase of k_D within the interval of [1, 1.2], and increases with the increase of k_D in the interval of [1.4, 2]. Thus, the dynamic field coefficient (k_D) is fixed at 1.2 for maximum evacuation efficiency.

Conformity parameter (k_M). According to the test results in Fig. 4 c, the evacuation time drops quickly with the increase of k_M in the interval of [1, 1.4]; it increases with k_M in the interval of [1.4, 1.9]; and it increases quickly with the increase of k_M in the interval of [1.9, 2]. Thus, the conformity parameter (k_M) is fixed at 1.2 for maximum evacuation efficiency.

4. RESULT ANALYSIS AND DISCUSSION

The attenuation coefficient (α), transmission coefficient (β), variance (σ^2), and threshold (E_0) of panic emotions were set to 0.9, 0.15, 0.05, and 0.7, respectively. The blue cells were adult cells, the black cells were companion cells, and the red cells were disadvantage cells. The pedestrian distributions under different time steps are shown in Fig. 5.

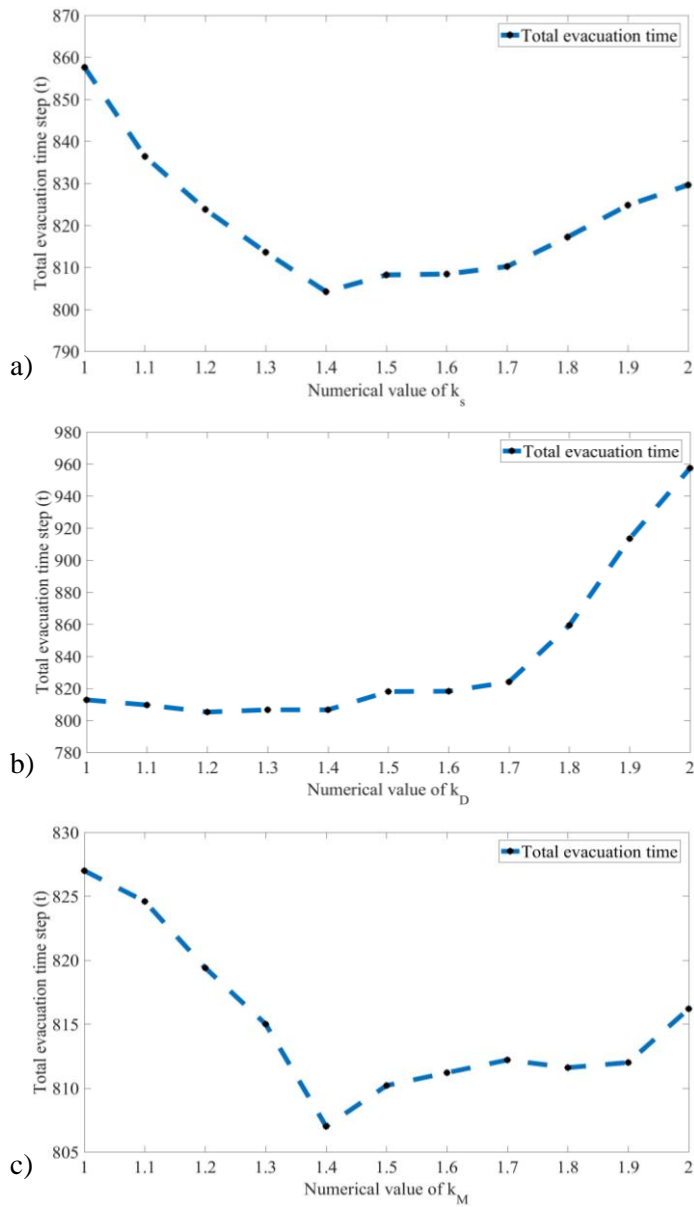


Figure 4: Relationship curve between average evacuation time and numerical values of k_s , k_D and k_M .

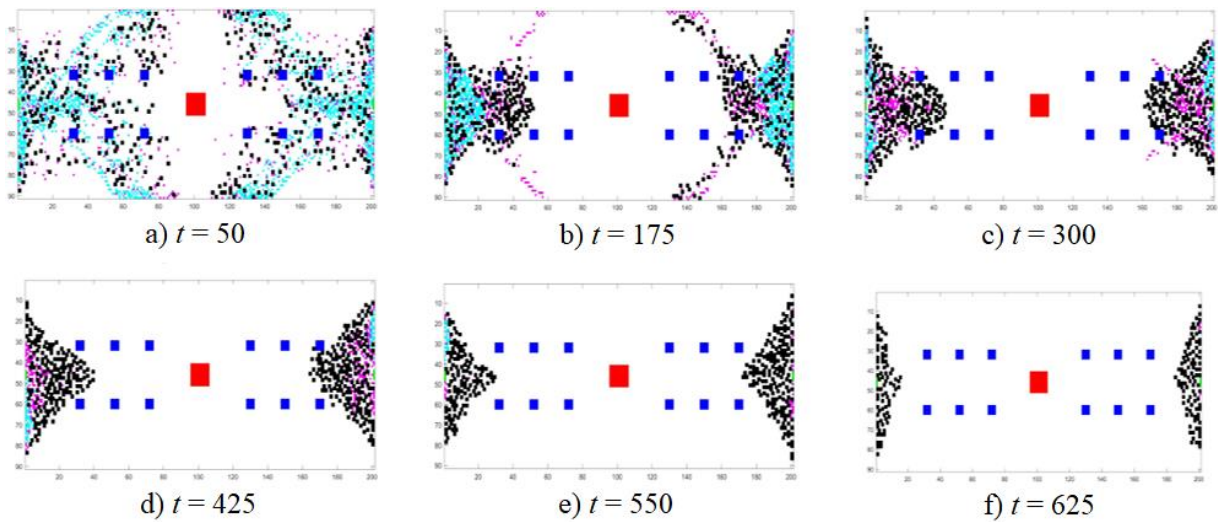


Figure 5: Pedestrian distribution maps under different time steps.

4.1 Influences of pedestrians

The influencing factors of pedestrians on evacuation results can be divided into the initial pedestrian density (ρ) and the companion ratio. The simulation process is shown in Fig. 6.

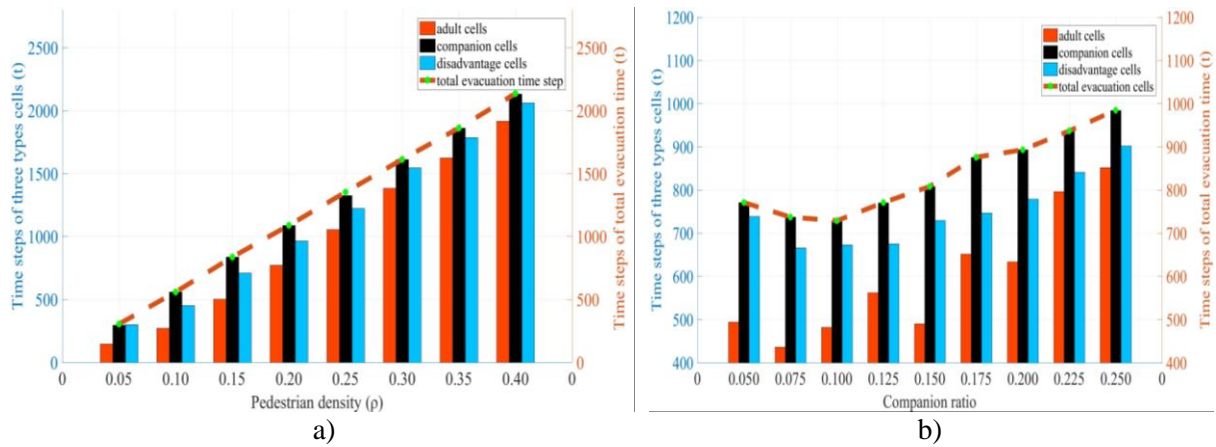


Figure 6: Relationship map between the influencing factors of pedestrians and evacuation time; a) initial pedestrian density (ρ), b) companion ratio.

Initial pedestrian density (ρ). As shown in Fig. 6 a, the total evacuation time has the same variation trend with pedestrian density. With the increase of pedestrian density in the evacuation area, the evacuation time also presents a linear growth trend. The greater the density of the evacuation, the less efficient the evacuation.

Companion ratio. As shown in Fig. 6 b, the proportion of evacuation time of adult cells in the total evacuation time generally increases with the companion ratio (m). Specifically, the evacuation time of companion cells and disadvantage cells is negatively related with the companion ratio in the interval of [0.05, 0.1], but it turns into a positive relationship with companion ratio in the interval of [0.1, 0.25]. The evacuation time of companion cells is basically consistent with the total evacuation time. When the companion ratio is 0.1, that is, adult cells : companion cells : disadvantage cells = 0.65 : 0.1 : 0.25. The evacuation takes the shortest time, valuing 728.8 time steps.

4.2 Influences of panic emotions

The simulation process of influences of panic emotions is shown in Fig. 7.

Attenuation coefficient of panic emotions (α). As shown in Fig. 7 a, the evacuation efficiency decreases gradually with the increase of α , but the total evacuation time increases gradually. When α is in the interval of [0.8, 0.85], the evacuation time increases to an extremely small extent with the increase of α , whereas evacuation efficiency declines slightly. In the interval of [0.85, 0.975], the evacuation time increases quickly with the increase of α , but the evacuation efficiency drops more obviously than that before.

In practical evacuation process, people often struggle with managing their emotions effectively. In other words, when the value of α is high, pedestrians are more likely to succumb to panic during evacuation, hindering their ability to make reasonable evacuation decisions and significantly reducing the efficiency of the evacuation. Conversely, if the crowd has strong emotional control, that is, if the numerical value of α is low, then the pedestrians are more likely to remain calm during the evacuation, allowing them to make reasonable decisions and significantly improving evacuation efficiency.

Transmission coefficient of panic emotions (β). As shown in Fig. 7 b, in the ranges of [0.025, 0.125] and [0.125, 0.2], the evacuation time presents a linear growth trend with the

increase of β . Moreover, the growth rate of the total evacuation time in the interval of [0.025, 0.125] is higher than that in the interval of [0.125, 0.2].

In the practical evacuation process, evacuees find it difficult to be affected by the panic emotions of others when β is low, which brings an extremely high evacuation efficiency. With the increase of β , evacuees are influenced increasingly by the panic emotions of others. The evacuation efficiency shows a fast linear reduction with the increase of β before reaching the boundary value of 0.1. After β exceeds 0.1, evacuation efficiency shows a linear reduction with the increase of β , but the reduction rate is lower than that in the interval of [0.025, 0.125].

Variance of panic emotions (σ^2). As shown in Fig. 7 c, the evacuation time decreases with the increase of σ^2 within the interval of [0.01, 0.05]. The evacuation time increases with the value of σ^2 within the interval of [0.05, 0.08]. The highest evacuation efficiency is achieved when σ^2 is 0.05, and the average evacuation time is 824.67 time steps.

In practical evacuation process, some pedestrians have poor emotions. They will cause a catfish effect in the evacuation process, which can improve evacuation efficiency throughout the process.

Threshold of panic emotion (E_0). As shown in Fig. 7 d, the evacuation time decreases with the increase of E_0 . When E_0 varies within the interval of [0.6, 0.75], the evacuation time declines minimally with the increase of E_0 .

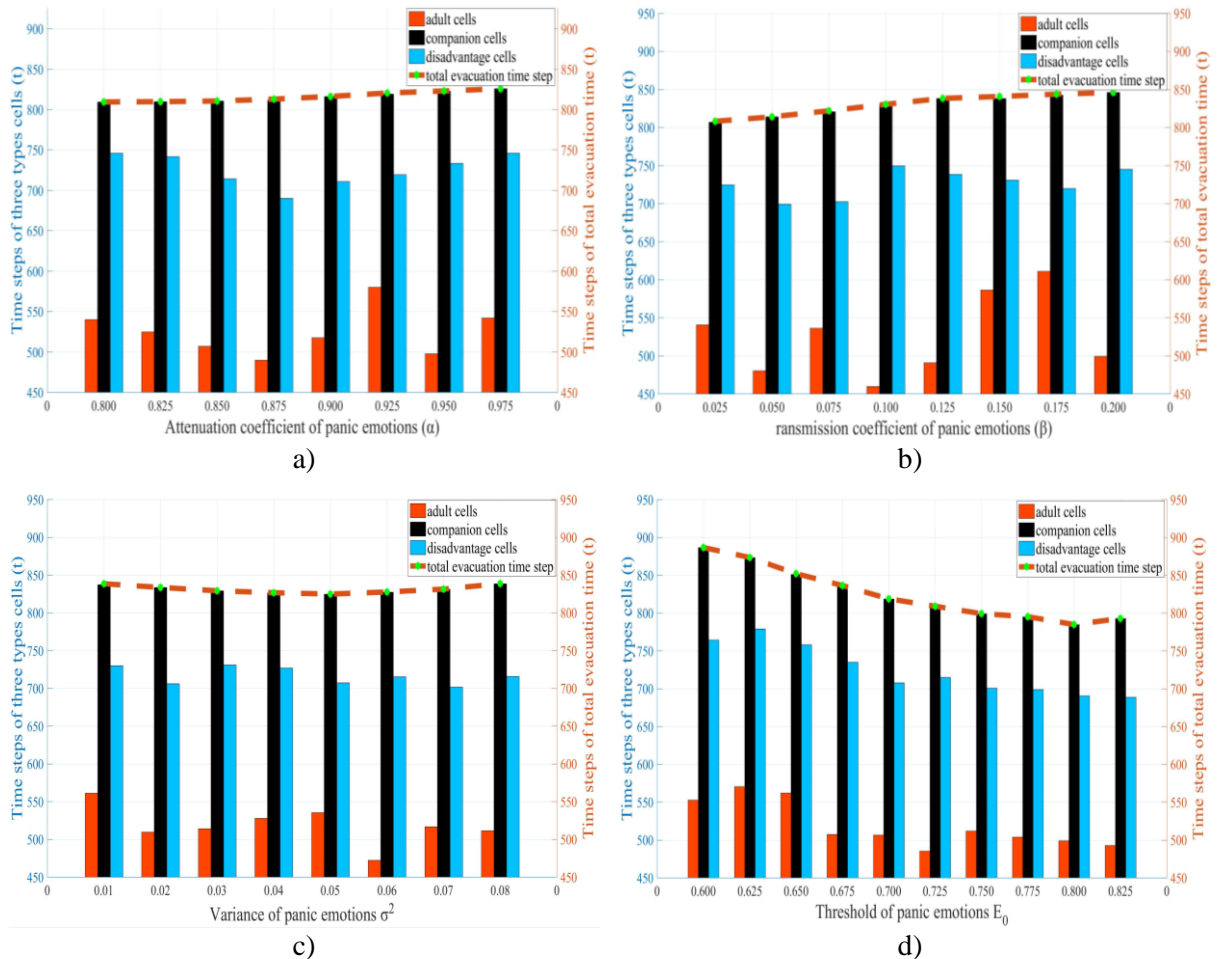


Figure 7: Relationship map between the influencing factors of panic emotions and evacuation time; a) attenuation coefficient of panic emotions α , b) transmission coefficient of panic emotions β , c) variance of panic emotions (σ^2), d) threshold of panic emotion (E_0).

The proportions of evacuation time of the three cell types under different values of E_0 in the total evacuation time all stay at relatively stable levels. The proportion of evacuation time of

adult cells fluctuates slightly around the mean of 62.85 %. The proportion of evacuation time of companion cells almost overlaps with the total evacuation time. The proportion of evacuation time of disadvantage cells fluctuates slightly around the mean of 87.65 %. Thus, E_0 has the same influencing ability on the three cell types in the evacuation process.

5. CONCLUSION

Based on the dynamic and static fields of the traditional cellular automaton model, this study enriches the description of evacuee conformity. According to practical scenarios, the concept of companion cells is introduced. With references to practical evacuation process, different time step lengths are given to unit moving distance of different cell types according to various walking speeds of different age groups. Based on this evacuation model, key attention is paid to influences of pedestrian number, structure, and panic emotions on the evacuation process. Large-scale simulations were conducted using the Matlab software. Some major conclusions could be drawn as follows:

1) A linear relationship exists between the total evacuation time and pedestrian density. With the increase of pedestrian density, the evacuation time of three cell types and the total evacuation time all achieve a linear growth with the increase of pedestrian density.

2) The evacuation time decreases initially and then increases with the companion ratio. When the companion ratio is lower than the threshold of 0.1, it can improve the overall evacuation efficiency by increasing the companion ratio. After the companion ratio exceeds 0.1, the overall space utilization during evacuation declines, thereby decreasing the overall evacuation efficiency. In other words, the highest evacuation efficiency is achieved when the ratio of adult cells : companion cells : disadvantage cells is 0.65 : 0.1 : 0.25.

3) People who have stronger control over their emotions during evacuation are more reasonable, which increases the overall evacuation efficiency. During evacuation, individuals shall try to remain reasonable as much as possible, adjust their mental state after suffering experiencing panic as soon as possible, calm down, and make the most correct evacuation decisions.

In summary, this study builds a cellular automaton evacuation model of dual-exit subway considering companion behaviours. The interactive behaviours and transmission of panic emotions of different age groups in the evacuation process are simulated. Limited by research conclusions, a simulation analysis based on Matlab software is performed in the case study. However, it lacks field test of evacuation, which shall be perfected in future studies.

REFERENCES

- [1] Chen, Y.-Y.; Chen, N.; Zhou, Y.-Y.; Wu, K.-H.; Zhang, W.-W. (2014). Pedestrian detection and tracking for counting applications in metro station, *Discrete Dynamics in Nature and Society*, Vol. 2014, Paper 712041, 11 pages, doi:[10.1155/2014/712041](https://doi.org/10.1155/2014/712041)
- [2] Mo, C. S.; Kim, S. G.; Kwon, Y. J.; Kang, K. S. (2015). Classification and standardized coding for urban railway casualty accident types and causes, *Journal of Civil and Environmental Engineering Research*, Vol. 35, No. 5, 1173-1177, doi:[10.12652/Ksce.2015.35.5.1173](https://doi.org/10.12652/Ksce.2015.35.5.1173)
- [3] Tsvirkun, A. D.; Rezhikov, A. F.; Filimonyuk, L. Y.; Samartsev, A. A.; Ivashchenko, V. A.; Bogomolov, A. S.; Kushnikov, V. A. (2022). System of integrated simulation of spread of hazardous factors of fire and evacuation of people from indoors, *Automation and Remote Control*, Vol. 83, No. 5, 692-705, doi:[10.1134/S0005117922050034](https://doi.org/10.1134/S0005117922050034)
- [4] Guo, X. Y.; Zeng, Z.; Li, M. X.; Fu, S. (2022). Simulation of aircraft cabin evacuation strategy based on exit flow equilibrium, *International Journal of Simulation Modelling*, Vol. 21, No. 2, 261-272, doi:[10.2507/IJSIMM21-2-601](https://doi.org/10.2507/IJSIMM21-2-601)

- [5] Zheng, Y.; Jia, B.; Li, X.-G.; Jiang, R. (2017). Evacuation dynamics considering pedestrians' movement behavior change with fire and smoke spreading, *Safety Science*, Vol. 92, 180-189, doi:[10.1016/j.ssci.2016.10.009](https://doi.org/10.1016/j.ssci.2016.10.009)
- [6] Qin, D.-H.; Duan, Y.-F.; Cheng, D.; Su, M.-Z.; Shao, Y.-B. (2020). An extended cellular automata model with modified floor field for evacuation, *Chinese Physics B*, Vol. 29, No. 9, Paper 098901, 9 pages, doi:[10.1088/1674-1056/abad1b](https://doi.org/10.1088/1674-1056/abad1b)
- [7] Ciallella, A.; Cirillo, E. N. M.; Curseu, P. L.; Muntean, A. (2018). Free to move or trapped in your group: mathematical modeling of information overload and coordination in crowded populations, *Mathematical Models and Methods in Applied Sciences*, Vol. 28, No. 9, 1831-1856, doi:[10.1142/S0218202518400079](https://doi.org/10.1142/S0218202518400079)
- [8] Pereira, L. A.; Burgarelli, D.; Duczmal, L. H.; Cruz, F. R. B. (2017). Emergency evacuation models based on cellular automata with route changes and group fields, *Physica A: Statistical Mechanics and its Applications*, Vol. 473, 97-110, doi:[10.1016/j.physa.2017.01.048](https://doi.org/10.1016/j.physa.2017.01.048)
- [9] Jahedinia, F.; Bagheri, M.; Naderan, A.; Bahramian, Z. (2023). Simulation of luggage-laden passengers' behavior in the evacuation process based on a floor field CA model case study: Tehran metro-rail transfer corridor, *Simulation*, Vol. 99, No. 7, 681-701, doi:[10.1177/00375497221140918](https://doi.org/10.1177/00375497221140918)
- [10] Mitsopoulou, M.; Dourvas, N. I.; Sirakoulis, G. C.; Nishinari, K. (2019). Spatial games and memory effects on crowd evacuation behavior with Cellular Automata, *Journal of Computational Science*, Vol. 32, 87-98, doi:[10.1016/j.jocs.2018.09.003](https://doi.org/10.1016/j.jocs.2018.09.003)
- [11] Geng, Z.; Li, X.; Kuang, H.; Bai, X.; Fan, Y. (2019). Effect of uncertain information on pedestrian dynamics under adverse sight conditions, *Physica A: Statistical Mechanics and its Applications*, Vol. 521, 681-691, doi:[10.1016/j.physa.2019.01.122](https://doi.org/10.1016/j.physa.2019.01.122)
- [12] Helbing, D.; Molnár, P. (1995). Social force model for pedestrian dynamics, *Physical Review E*, Vol. 51, No. 5, 4282-4286, doi:[10.1103/PhysRevE.51.4282](https://doi.org/10.1103/PhysRevE.51.4282)
- [13] Helbing, D.; Farkas, I.; Vicsek, T. (2000). Simulating dynamical features of escape panic, *Nature*, Vol. 407, No. 6803, 487-490, doi:[10.1038/35035023](https://doi.org/10.1038/35035023)
- [14] Li, Z.; Wen, Y.; Zhao, L.; Dong, Y. (2020). Modeling human evacuating behavior in limited space based on Cellular Automata model, *Complexity*, Vol. 2020, Paper 7238469, 11 pages, doi:[10.1155/2020/7238469](https://doi.org/10.1155/2020/7238469)
- [15] Gokce, S.; Cetin, A.; Kibar, R. (2018). Investigating pedestrian evacuation using ant algorithms, *Pramana – Journal of Physics*, Vol. 91, No. 5, Paper 62, 11 pages, doi:[10.1007/s12043-018-1621-2](https://doi.org/10.1007/s12043-018-1621-2)
- [16] Gwizdała, T. M. (2015). Some properties of the floor field cellular automata evacuation model, *Physica A: Statistical Mechanics and its Applications*, Vol. 419, 718-728, doi:[10.1016/j.physa.2014.10.070](https://doi.org/10.1016/j.physa.2014.10.070)
- [17] Miyagawa, D.; Ichinose, G. (2020). Cellular automaton model with turning behavior in crowd evacuation, *Physica A: Statistical Mechanics and its Applications*, Vol. 549, Paper 124376, 8 pages, doi:[10.1016/j.physa.2020.124376](https://doi.org/10.1016/j.physa.2020.124376)
- [18] Zuriguel, I.; Janda, A.; Garcimartín, A.; Lozano, C.; Arévalo, R.; Maza, D. (2011). Silo clogging reduction by the presence of an obstacle, *Physical Review Letters*, Vol. 107, No. 27, Paper 278001, 5 pages, doi:[10.1103/PhysRevLett.107.278001](https://doi.org/10.1103/PhysRevLett.107.278001)
- [19] Yanagisawa, D.; Nishi, R.; Tomoeda, A.; Ohtsuka, K.; Kimura, A.; Suma, Y.; Nishinari, K. (2010). Study on efficiency of evacuation with an obstacle on hexagonal cell space, *SICE Journal of Control, Measurement, and System Integration*, Vol. 3, No. 6, 395-401, doi:[10.9746/jcmsi.3.395](https://doi.org/10.9746/jcmsi.3.395)
- [20] Song, W.; Yu, Y.; Fan, W.; Zhang, H. (2005). A cellular automata evacuation model considering friction and repulsion, *Science in China (Series E: Engineering & Materials Science)*, Vol. 35, No. 7, 725-736, doi:[10.1360/03ye0486](https://doi.org/10.1360/03ye0486)
- [21] Yi, J.; Pan, S.; Chen, Q. (2020). Simulation of pedestrian evacuation in stampedes based on a cellular automaton model, *Simulation Modelling Practice and Theory*, Vol. 104, Paper 102147, 14 pages, doi:[10.1016/j.simpat.2020.102147](https://doi.org/10.1016/j.simpat.2020.102147)
- [22] Feliciani, C.; Nishinari, K. (2016). An improved cellular automata model to simulate the behavior of high density crowd and validation by experimental data, *Physica A: Statistical Mechanics and its Applications*, Vol. 451, 135-148, doi:[10.1016/j.physa.2016.01.057](https://doi.org/10.1016/j.physa.2016.01.057)

- [23] Allen, L. J. S.; Burgin, A. M. (2020). Comparison of deterministic and stochastic SIS and SIR models in discrete time, *Mathematical Biosciences*, Vol. 163, No. 1, 1-33, doi:[10.1016/S0025-5564\(99\)00047-4](https://doi.org/10.1016/S0025-5564(99)00047-4)
- [24] Hill, A. L.; Rand, D. G.; Nowak, M. A.; Christakis, N. A. (2010). Emotions as infectious diseases in a large social network: the SISa model, *Proceedings of the Royal Society B: Biological Science*, Vol. 277, No. 1701, 3827-3835, doi:[10.1098/rspb.2010.1217](https://doi.org/10.1098/rspb.2010.1217)
- [25] Fu, L.; Song, W.; Lv, W.; Lo, S. (2014). Simulation of emotional contagion using modified SIR model: a cellular automaton approach, *Physica A: Statistical Mechanics and its Applications*, Vol. 405, 380-391, doi:[10.1016/j.physa.2014.03.043](https://doi.org/10.1016/j.physa.2014.03.043)
- [26] Wu, G.; Peng, C.; Liao, T. W. (2018). Research on edges immunization strategy for complex network based on SIS-CA model, *Procedia Manufacturing*, Vol. 17, 1065-1072, doi:[10.1016/j.promfg.2018.10.079](https://doi.org/10.1016/j.promfg.2018.10.079)